Time-dependent potential-functional embedding theory

Chen Huang,[1,a)] Florian Libisch,[2] Qing Peng,[3] and Emily A. Carter[4,b)]
[1]*Theoretical Division, Los Alamos National Laboratory, New Mexico 87544, USA*
[2]*Institute for Theoretical Physics, Vienna University of Technology, Wiedner Hauptstraße 8-10/136, 1040 Vienna, Austria*
[3]*Department of Mechanical, Aerospace and Nuclear Engineering, Rensselaer Polytechnic Institute, Troy, New York 12180, USA*
[4]*Department of Mechanical and Aerospace Engineering and Chemistry, Program in Applied and Computational Mathematics, and Andlinger Center for Energy and the Environment, Princeton University, Princeton, New Jersey 08544, USA*

(Received 16 January 2014; accepted 13 March 2014; published online 31 March 2014)

We introduce a time-dependent potential-functional embedding theory (TD-PFET), in which atoms are grouped into subsystems. In TD-PFET, subsystems can be propagated by different suitable time-dependent quantum mechanical methods and their interactions can be treated in a seamless, first-principles manner. TD-PFET is formulated based on the time-dependent quantum mechanics variational principle. The action of the total quantum system is written as a functional of the time-dependent embedding potential, i.e., a potential-functional formulation. By exploiting the Runge-Gross theorem, we prove the uniqueness of the time-dependent embedding potential under the constraint that all subsystems share a common embedding potential. We derive the integral equation that such an embedding potential needs to satisfy. As proof-of-principle, we demonstrate TD-PFET for a Na_4 cluster, in which each Na atom is treated as one subsystem and propagated by time-dependent Kohn-Sham density functional theory (TDDFT) using the adiabatic local density approximation (ALDA). Our results agree well with a direct TDDFT calculation on the whole Na_4 cluster using ALDA. We envision that TD-PFET will ultimately be useful for studying ultrafast quantum dynamics in condensed matter, where key regions are solved by highly accurate time-dependent quantum mechanics methods, and unimportant regions are solved by faster, less accurate methods.
© *2014 AIP Publishing LLC*. [http://dx.doi.org/10.1063/1.4869538]

I. INTRODUCTION

Time-dependent quantum mechanics forms the cornerstone for our understanding and prediction of electron dynamics in materials, e.g., exciton creation and separation in solar cells,[1] surface-enhanced Raman spectroscopy,[2] and biosensing based on exciton-plasmon interactions,[3] to name only a few applications. However, sophisticated time-dependent correlated-wavefunction (TDCW) techniques such as the time-dependent coupled cluster method[4] are prohibitively expensive. To correctly describe the sequential double-ionization of helium even requires explicit treatment of the full time-dependent two-particle Schrödinger equation.[5] Such an approach is unfeasible already for three electrons. To efficiently propagate the time-dependent Schrödinger equation, time-dependent density functional theory (TDDFT) based on the Runge-Gross theorem was introduced.[6] Practical applications of TDDFT employing the adiabatic local density approximation (ALDA) unfortunately share many problems with ground state time-independent DFT,[7,8] such as the self-interaction error[9] and the lack of a derivative discontinuity in the exchange-correlation (XC) potential.[10] Additionally, constructing a time-dependent XC functional with memory is very challenging.[11] To overcome these difficulties, herein we formulate a theory capable of describing a region (or regions) of interest in a complex system with an accurate *ab initio* time-dependent quantum mechanics method. A less expensive, lower-level method could then be used to treat the surrounding regions, giving rise to a time-dependent embedding theory.

Various embedding theories have been developed in the past for time-independent quantum systems. For instance, embedding methods employing the Green's function were developed to study chemisorption[12–14] and defects in semiconductors.[15] Inglesfield solved for the region of interest utilizing the Green's function on its boundary.[16] Density-functional embedding theory (DFET), which extends DFT from a single quantum system to multiple quantum systems, is in principle exact, and has been extensively developed in the last two decades. In DFET, one partitions the total electron density into subsystem electron densities. The interaction (embedding potential) between subsystems is calculated according to a subsystem reformulation of DFT.[17–20] The embedding potential is often evaluated with the help of approximate kinetic energy density functionals (KEDFs).[17–20] To improve the accuracy of embedding potential, exact KEDF potential can calculated by directly inverting the Kohn-Sham equations,[21–24] or by level shifting subsystem orbitals.[25] It has recently been realized that the uniqueness of the embedding potential is essential for making DFET tractable.[26,27] One common way to perform DFET is DFT-in-DFT embedding,

a)chenh@lanl.gov
b)eac@princeton.edu

 © 2014 AIP Publishing LLC

This article is copyrighted as indicated in the article. Reuse of AIP content is subject to the terms at: http://scitation.aip.org/termsconditions. Downloaded to IP: 66.67.101.221 On: Mon, 31 Mar 2014 14:59:43

in which all subsystems are treated within DFT.[17–19,25] In CW-in-DFT embedding, key regions are treated using a CW method, while the environment is treated using DFT.[20,27–33] CW-in-DFT embedding using spin-dependent embedding potentials has also been demonstrated.[34] We recently introduced a self-consistent potential-functional embedding theory (PFET), in which one directly minimizes the total energy with respect to the embedding potential (a unique property for a given system partitioning) instead of with respect to the electron densitiy.[35] PFET makes it possible to perform seamless embedding simulations for molecules and materials in a divide-and-conquer manner, allowing charge transfer between subsystems. Reviews of DFET[36,37] and PFET,[38] as well as an overview of various embedding schemes are available.[36]

For time-dependent quantum systems, Inglesfield developed a time-dependent embedding theory[39,40] that matches one-electron wavefunctions across adjacent regions. Several time-dependent embedding theories have been developed to study the interactions between molecules and metals: metals often have been represented with simplified models,[41] or the interactions between molecules and metals have been described by classical electrodynamics.[42–47] More sophisticated quantum mechanical approaches have appeared recently. By treating the plasmons in metals as a perturbation, Masiello and Schatz developed a many-body perturbation theory approach to simulate surface-enhanced Raman spectroscopy.[48] Chen *et al.*[49] thereafter constructed a multi-scale theory in which the scattering response function of the environment was calculated and then used as input for subsequent time-dependent simulations of molecules. They assumed that the scattering response function was uniformly distributed around the molecule.

Excitation energies in molecules are now routinely calculated based on TD-DFT linear response theory.[50,51] Subsystem formulation of TD-DFT linear response has also been extensively developed.[52–57] In the present work, we introduce a flexible subsystem formulation of time-dependent quantum processes that is not restricted to the linear response regime: general time-dependent potential-functional embedding theory (TD-PFET), which partitions the total system into several subsystems. In the simplest case, we partition a system subject to a time-dependent external potential into two subsystems I (a region of interest) and II (its environment) [Fig. 1(a)]. It is often unfeasible to treat a total system using a highly accurate quantum mechanics method due to very high computational cost. One goal of TD-PFET would be to study subsystem I using an accurate time-dependent quantum mechanics method, and to treat the subsystem II using a less accurate but faster method. By employing such a divide-and-conquer approach, we may be able to gain a reliable picture of the quantum dynamics in subsystem I, while limiting the computational cost. Currently, we do not permit charge transfer between subsystems but restrict ourselves to intra-subsystem excitations.

The basic idea in TD-PFET is to replace the interaction between subsystems with a time-dependent embedding potential. Each subsystem is propagated with the embedding potential as an additional time-dependent external potential. The action of the total system is formulated as a functional of the time-dependent embedding potential, which is solved for by satisfying the time-dependent variational principle. Unlike Inglesfield's approach,[39] we do not explicitly define geometric boundaries to partition the total system into subsystems. Upon grouping atoms into subsystems, the partitioning of the total time-dependent electron density is automatically achieved. The present work naturally extends our recent work on PFET[35] to time-dependent quantum phenomena.

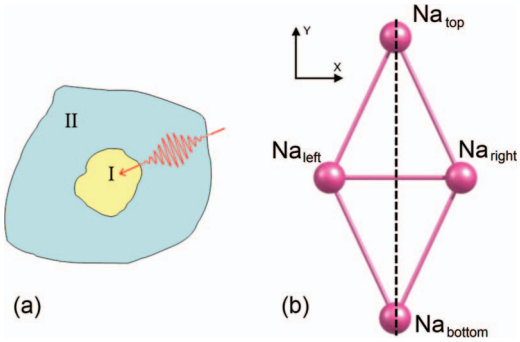

FIG. 1. (a) Schematic of the total system under an external time-dependent field such as a laser. In TD-PFET, the system is partitioned into subsystems, here for illustration just two of them, I and II. They can then be treated by different time-dependent quantum mechanics methods if desirable. (b) Geometry of a planar Na_4 cluster in the x-y plane. The laser points in the y direction. The distance between Na_{top} and Na_{bottom} is 6.51 Å. The distance between the Na_{left} and Na_{right} is 3.05 Å. In our TD-PFET simulations, each Na atom is treated as one subsystem.

TD-PFET presented here provides an *ab initio*, self-consistent, and seamless framework to study different regions of materials with different time-dependent quantum mechanics methods. For example, using TD-PFET, it will become possible to study multiple regions of interest in materials and molecules with suitable TDCW methods, while treating the environment with lower-level and faster time-dependent quantum mechanics methods, such as TDDFT/ALDA. We refer to such a scheme as TDCW-in-TDDFT embedding. Here, in addition to formulating the theory, as a first proof of principle we demonstrate TDDFT-in-TDDFT embedding for a Na_4 cluster in the presence of a laser field, with each Na atom treated as a subsystem within TDDFT/ALDA. We show that our TD-PFET is able to reproduce the time evolution of the dipole moment and other time-dependent quantities in good agreement with a benchmark TDDFT/ALDA calculation on the entire Na_4 cluster.

This paper is organized as follows. We present the formalism of TD-PFET based on the quantum mechanics variational principle. An integral equation describing the time-evolution of the time-dependent embedding potential is then derived. The uniqueness of this time-dependent embedding potential is proved in the Appendix. We discuss how to approximate several key terms in the integral equation to make it easier to solve, and show how to greatly simplify it for the case of TDDFT/ALDA-in-TDDFT/ALDA embedding. To calculate the time-dependent Kohn-Sham effective potential for a given v-representable time-dependent electron density, we develop a penalty-function based method. We demonstrate our TD-PFET on a Na_4 cluster, where each Na atom is treated as one subsystem. Finally we compare TD-PFET to a recently

This article is copyrighted as indicated in the article. Reuse of AIP content is subject to the terms at: http://scitation.aip.org/termsconditions. Downloaded to IP: 66.67.101.221 On: Mon, 31 Mar 2014 14:59:43

developed "fragment-time-dependent density functional theory" and offer concluding remarks.

II. THEORY

A. Formalism of TD-PFET

We consider a time-dependent quantum system that contains M atoms with coordinates $\vec{R}_1 \ldots \vec{R}_M$ and nuclear charges $Z_1 \ldots Z_M$. The system contains M_e electrons and is driven by an external time-dependent potential $v_{td}(\vec{r}, t)$. The electronic Hamiltonian is

$$\hat{H}_{tot}(t) = -\sum_{i=1}^{M_e} \frac{1}{2}\nabla_i^2 - \sum_{i=1}^{M_e}\sum_{j=1}^{M} \frac{Z_j}{|\vec{r}_i - \vec{R}_j|} + \sum_{i=1}^{M_e}\sum_{j<i}^{M_e} \frac{1}{|\vec{r}_i - \vec{r}_j|} + \sum_{i=1}^{M_e} v_{td}(\vec{r}_i, t). \quad (1)$$

In TD-PFET, we partition the total system into N subsystems by grouping the ionic potentials of all M atoms into $K = 1, \ldots, N$ subsystems, each containing M_{eK} electrons and M_K atoms. Static PFET allows for adjusting the M_{eK} by letting all subsystems share a common chemical potential. In the time-dependent embedding case, the system is not in equilibrium, therefore we no longer have a constant chemical potential over all space. The current formalism thus uses fixed subsystem electron numbers M_{eK} during TD-PFET simulations, which thus prevents TD-PFET from studying electron transfer between subsystems.

The Hamiltonian of subsystem K is defined as

$$\hat{H}_K(t) = -\sum_{i=1}^{M_{eK}} \frac{1}{2}\nabla_i{}^2 - \sum_{i=1}^{M_{eK}}\sum_{j=1}^{M_K} \frac{Z_j}{|\vec{r}_i - \vec{R}_j|} + \sum_{i=1}^{M_{eK}}\sum_{j<i}^{M_{eK}} \frac{1}{|\vec{r}_i - \vec{r}_j|} + \sum_{i=1}^{M_{eK}} (v_{td}(\vec{r}_i, t) + u_{emb,K}(\vec{r}_i, t)), \quad (2)$$

where $\sum_{K=1}^{N} M_{eK} = M_e$ and $\sum_{K=1}^{N} M_K = M$. In Eq. (2), we have added the embedding potential $u_{emb,K}(\vec{r}, t)$ to represent the interaction between subsystem K and the rest of the system. In principle, $u_{emb,K}(\vec{r}, t)$ is subsystem-dependent. However, similar to our previous work on PFET,[35] we apply the constraint that all subsystems share a *common* time-dependent embedding potential (denoted as $u_{emb}(\vec{r}, t)$), i.e., we replace $u_{emb,K}(\vec{r}, t)$ with $u_{emb}(\vec{r}, t)$ in Eq. (2). As shown in the Appendix, such a constraint guarantees the uniqueness of $u_{emb}(\vec{r}, t)$.

The Runge-Gross theorem ensures that the time evolution of the total system is completely determined by $\rho_{tot}(\vec{r}, t)$ and the initial many-body wavefunction $|\Psi_{tot}(t = 0)\rangle$ of the total system. In our TD-PFET ansatz, subsystem electron densities $\{\rho_K(\vec{r}, t)\}$ and the total electron density $\rho_{tot}(\vec{r}, t) = \sum_{K=1}^{N} \rho_K(\vec{r}, t)$ are determined by $u_{emb}(\vec{r}, t)$. Together, $u_{emb}(\vec{r}, t)$ and $|\Psi_{tot}(t = 0)\rangle$ determine the time evolution of the total system, which makes all quantities in TD-PFET functionals of $u_{emb}(\vec{r}, t)$ and $|\Psi_{tot}(t = 0)\rangle$; i.e., we follow the potential-functional formalism introduced in PFET.[35]

The central question now becomes how to solve for such a time-dependent embedding potential. To derive the integral equation that $u_{emb}(\vec{r}, t)$ is required to satisfy, we decompose the action of the total system as

$$A_{tot} = \sum_K A_K + \left(A_{tot} - \sum_K A_K \right), \quad (3)$$

where A_{tot} and A_K are respectively the actions of the total system and subsystem K, defined in real-time (from $t = 0$ to $t = T$)

$$A_{tot}[u_{emb}] = \int_0^T dt' \langle \Psi_{tot}(t')[u_{emb}] | i\partial_{t'} - \hat{H}_{tot}(t') | \Psi_{tot}(t')[u_{emb}] \rangle \quad (4)$$

and

$$A_K[u_{emb}] = \int_0^T dt' \langle \Psi_K(t')[u_{emb}] | i\partial_{t'} - \hat{H}_K(t') | \Psi_K(t')[u_{emb}] \rangle. \quad (5)$$

The many-body wavefunction and Hamiltonian of the total system (of subsystem K) are respectively $|\Psi_{tot}(t)\rangle$ and $\hat{H}_{tot}(t)(|\Psi_K(t)\rangle$ and $\hat{H}_K(t))$. As discussed above $|\Psi_K(t)\rangle$ is determined by $u_{emb}(\vec{r}, t)$. $|\Psi_{tot}(t)\rangle$ is a functional of the total electron density $\rho_{tot}(\vec{r}, t)$ which is the superposition of all subsystem electron densities $\rho_K(\vec{r}, t)$. Since $\rho_K(\vec{r}, t)$ is a functional of $u_{emb}(\vec{r}, t)$, $|\Psi_{tot}(t)\rangle$ is an implicit functional of $u_{emb}(\vec{r}, t)$. In Eq. (3), the interaction action A_{int} is formally defined as

$$A_{\text{int}} \equiv A_{tot} - \sum_K A_K. \quad (6)$$

In practical TD-PFET simulations, A_{int} needs to be approximated, as we discuss in Sec. II B.

In our previous time-independent embedding theory, i.e., PFET,[35] the embedding potential was solved for by directly minimizing the total energy with respect to the embedding potential. However, such a method cannot be used for TD-PFET, because there is no variational principle for the total system's action with respect to the embedding potential, i.e., $\frac{\delta A_{tot}}{\delta u_{emb}} \neq 0$.[58] This can be understood by writing down the variation of A_{tot} with respect to $\delta u_{emb}(\vec{r}, t)$,[58]

$$\begin{aligned}
\delta A_{tot} &= \int_0^T dt' \langle \delta\Psi_{tot}(t') | i\partial_{t'} - \hat{H}_{tot}(t') | \Psi_{tot}(t') \rangle \\
&\quad + \int_0^T dt' \langle \Psi_{tot}(t') | i\partial_{t'} - \hat{H}_{tot}(t') | \delta\Psi_{tot}(t') \rangle, \\
&= \int_0^T dt' \langle \delta\Psi_{tot}(t') | i\partial_{t'} - \hat{H}_{tot}(t') | \Psi_{tot}(t') \rangle \\
&\quad + \int_0^T dt' \langle [i\partial_{t'} - \hat{H}_{tot}(t')] \Psi_{tot}(t') | \delta\Psi_{tot}(t') \rangle \\
&\quad + i \langle \Psi_{tot}(t') \mid \delta\Psi_{tot}(t') \rangle |_0^T, \quad (7)
\end{aligned}$$

where $\delta\Psi_{tot}(t)$ is caused by a variation of $u_{emb}(\vec{r}, t)$ at an earlier time. For the second equality in Eq. (7), an integration by

This article is copyrighted as indicated in the article. Reuse of AIP content is subject to the terms at: http://scitation.aip.org/termsconditions. Downloaded to IP: 66.67.101.221 On: Mon, 31 Mar 2014 14:59:43

parts is performed,

$$\int_0^T dt' \langle \Psi_{tot}(t')| i\partial_{t'} |\delta\Psi_{tot}(t')\rangle$$

$$= i\langle \Psi_{tot}(t')|\delta\Psi_{tot}(t')\rangle|_0^T - i\int_0^T dt' \langle \partial_{t'}\Psi_{tot}(t')|\delta\Psi_{tot}(t')\rangle.$$

The correct $u_{emb}(\vec{r},t)$ yields the $|\Psi_{tot}(t)\rangle$ that satisfies the time-dependent Schrödinger equation, i.e., $(i\partial_t - \hat{H}_{tot}(t))\Psi_{tot}(t) = 0$. Consequently, together with $\delta\Psi_{tot}(t=0) = 0$, Eq. (7) is reduced to

$$\frac{\delta A_{tot}[u_{emb}]}{\delta u_{emb}(\vec{r},t)} = i\left\langle \Psi_{tot,T}[u_{emb}] \middle| \frac{\delta\Psi_{tot,T}[u_{emb}]}{\delta u_{emb}(\vec{r},t)} \right\rangle, \tag{8}$$

for any $t \le T$. $\Psi_{tot,T}$ is short for $\Psi_{tot}(t=T)$. In Eq. (8), we note that the variation of A_{tot} with respect to the correct $u_{emb}(\vec{r},t)$ does not vanish, but is related to a boundary term evaluated at $t = T$. As pointed out in Ref. 58, it is this boundary term that preserves causality in TDDFT. Equation (8) is therefore a necessary condition for finding the correct $u_{emb}(\vec{r},t)$ to yield the $|\Psi_{tot}(t)\rangle$ satisfying $(i\partial_t - \hat{H}_{tot}(t))\Psi_{tot}(t) = 0$.

We now prove that Eq. (8) is also a *sufficient* condition. Let's assume that $u_{emb}(\vec{r},t)$ yields a different v-representable $\Psi_{tot}{}'(t)$ satisfying $(i\partial_t - \hat{H}_{tot}{}'(t))\Psi_{tot}{}'(t) = 0$, with $\hat{H}_{tot}{}'(t)$ being different from $\hat{H}_{tot}(t)$. Since Eq. (8) holds for $u_{emb}(\vec{r},t)$ for $0 \le t \le T$, Eq. (7) reduces to

$$\int_0^T dt' \langle \delta\Psi_{tot}{}'(t')| i\partial_{t'} - \hat{H}_{tot}(t')|\Psi_{tot}{}'(t')\rangle + c.c. = 0, \tag{9}$$

for any variation $\delta u_{emb}(\vec{r},t)$, where *c.c.* is short for the complex conjugate. Denoting $\Delta\hat{V}(t) = \hat{H}'_{tot}(t) - \hat{H}_{tot}(t)$, Eq. (9) becomes

$$0 = \int_0^T dt' \langle \delta\Psi_{tot}{}'(t')|\Delta\hat{V}(t')|\Psi_{tot}{}'(t')\rangle + c.c.$$

$$= \int_0^T dt' \int dr'^3 \delta\rho_{tot}{}'(\vec{r}',t')\Delta V(\vec{r}',t'), \tag{10}$$

with $\rho_{tot}{}'(\vec{r},t)$ being the electron density associated with $\Psi_{tot}{}'(t)$. Our goal is to show that $\Psi_{tot}{}'(t)$ is the solution of $(i\partial_t - \hat{H}_{tot}(t))\Psi_{tot}{}'(t) = 0$, i.e., $\Delta V(\vec{r},t)$ is a time-dependent constant $[\Delta V(\vec{r},t) \equiv Q(t)]$, which requires that $\delta\rho_{tot}{}'(\vec{r},t)$ in Eq. (10) can be arbitrary.

As shown in the Appendix, $\rho_{tot}{}'(\vec{r},t)$ determines $u_{emb}(\vec{r},t)$ up to a time-dependent function $c(t)$. We focus on a subset of $u_{emb}(\vec{r},t)$, denoted as U^g_{emb}, in which such an arbitrary gauge freedom $c(t)$ is removed: $\int dr^3 u^g_{emb}(\vec{r},t) = 0$ and $\int dr^3 \delta u^g_{emb}(\vec{r},t) = 0$ for any t and any $u^g_{emb} \in \mathrm{U}^g_{emb}$. We can map $\delta\rho_{tot}{}'(t)$ to $\delta u^g_{emb}(\vec{r},t)$ by the time-dependent linear response

$$\delta\rho_{tot}{}'(\vec{r},t) = \int_0^t dt' \int d\vec{r}' \chi(\vec{r},t;\vec{r}',\vec{t}')\delta u^g_{emb}(\vec{r}',t'). \tag{11}$$

To show that $\delta\rho_{tot}{}'(\vec{r},t)$ in Eq. (10) can be arbitrary, we need to prove that χ is invertible. We show this for the case of discrete space and time variables. We discretize both the spatial and time coordinates as $\{r_1, r_2, \ldots, r_M\}$ and $\{t_1, t_2, \ldots, t_D\}$, respectively. Equation (11) then reduces to the matrix representation

$$\boldsymbol{\delta\rho_{tot}}' = \boldsymbol{\chi}\,\boldsymbol{\delta u^g_{emb}},$$

where

$$\boldsymbol{\delta\rho_{tot}}' = \left[\delta\rho_{tot\,r_1,t_1}{}', \delta\rho_{tot\,r_2,t_1}{}', \ldots, \delta\rho_{tot\,r_M,t_1}{}', \ldots, \delta\rho_{tot\,r_1,t_D}{}', \delta\rho_{tot\,r_2,t_D}{}', \ldots, \delta\rho_{tot\,r_M,t_D}{}'\right]^T,$$

$$\boldsymbol{\delta u^g_{emb}} = \left[\delta u^g_{emb\,r_1,t_1}, \delta u^g_{emb\,r_2,t_1}, \ldots, \delta u^g_{emb\,r_M,t_1}, \ldots, \delta u^g_{emb\,r_1,t_D}, \delta u^g_{emb\,r_2,t_D}, \ldots, \delta u^g_{emb\,r_M,t_D}\right]^T,$$

$$\boldsymbol{\chi} = \begin{bmatrix} \chi_{t_1t_1} & \mathbf{0} & \cdots & \mathbf{0} \\ \chi_{t_2t_1} & \chi_{t_2t_2} & \cdots & \mathbf{0} \\ \vdots & \vdots & \ddots & \mathbf{0} \\ \chi_{t_Dt_1} & \chi_{t_Dt_2} & \cdots & \chi_{t_Dt_D} \end{bmatrix},$$

$$\boldsymbol{\chi_{t_it_j}} = \begin{bmatrix} \chi_{r_1t_i,r_1t_j} & \chi_{r_1t_i,r_2t_j} & \cdots & \chi_{r_1t_i,r_Mt_j} \\ \chi_{r_2t_i,r_1t_j} & \chi_{r_2t_i,r_2t_j} & \cdots & \chi_{r_2t_i,r_Mt_j} \\ \vdots & \vdots & \ddots & \vdots \\ \chi_{r_Mt_i,r_1t_j} & \chi_{r_Mt_i,r_2t_j} & \cdots & \chi_{r_Mt_i,r_Mt_j} \end{bmatrix} \quad \text{for } t_i \ge t_j.$$

If the null space of $\boldsymbol{\chi}$ is non-empty, a nonzero $\mathbf{v} \in \mathrm{U}^g_{emb}$ would exist such that $\boldsymbol{\chi}\mathbf{v} = \mathbf{0}$, due to the fact that the linearly independent basis in U^g_{emb} is of the same dimension as $\boldsymbol{\chi}$, i.e., $D \times M$. Thus both $\boldsymbol{\delta u^g_{emb}}$ and $(\boldsymbol{\delta u^g_{emb}} + \mathbf{v})$ would give the same $\boldsymbol{\delta\rho_{tot}}'$, which is contradictory to the one-to-one mapping between $u^g_{emb}(\vec{r},t)$ and $\rho_{tot}{}'(\vec{r},t)$ proved in the Appendix. Consequently, the linear response matrix $\boldsymbol{\chi}$ is of full rank $D \times M$ and invertible. Any arbitrary $\boldsymbol{\delta\rho_{tot}}'$ can then be obtained by $\boldsymbol{\delta u^g_{emb}} = \boldsymbol{\chi}^{-1}\boldsymbol{\delta\rho_{tot}}'$, which indicates that Eq. (10) can only hold for $\Delta V(\vec{r},t) = 0$. We have thus proven that Eq. (8) is a *sufficient* condition for solving for the correct $u_{emb}(\vec{r},t)$ for the case of discretized spatial and time coordinates. Since both A_{tot} and $\Psi_{tot,T}$ are implicit functionals of $u_{emb}(\vec{r},t)$, Eq. (8) is the integral equation for $u_{emb}(\vec{r},t)$, which

This article is copyrighted as indicated in the article. Reuse of AIP content is subject to the terms at: http://scitation.aip.org/termsconditions. Downloaded to IP: 66.67.101.221 On: Mon, 31 Mar 2014 14:59:43

is the central result of this work. The uniqueness of $u_{emb}(\vec{r},t)$ is proven in the Appendix.

The embedding potential $u_{emb}(\vec{r},t)$, obtained from Eq. (8), is a local function of time t and spatial coordinate $\vec{r}$. If no approximation is used in solving Eq. (8), $u_{emb}(\vec{r},t)$ does in principle have "memory": $u_{emb}(\vec{r},t)$ is determined by the total electron density in the past and the many-body wavefunction at $t=0$. This is similar to the time-dependent Kohn-Sham effective potential, which is also a local function of time and spatial coordinates, but nevertheless, in principle, has the correct "memory."

By a procedure similar to the derivation of Eq. (8), one can show that for subsystem K, the variation of A_K with $u_{emb}(\vec{r},t)$ is given by

$$\frac{\delta A_K}{\delta u_{emb}(\vec{r},t)} = i\left\langle \Psi_{K,T}\left| \frac{\delta \Psi_{K,T}}{\delta u_{emb}(\vec{r},t)}\right\rangle - \rho_K(\vec{r},t), \tag{12}$$

where ρ_K appears due to the $u_{emb,K}$ term in H_K [see Eq. (2)]. Equation (12) will be used in Secs. II B–II D.

B. Possible approximations in TD-PFET calculations

The goal of TD-PFET is to propagate each subsystem with a suitable time-dependent quantum mechanics method with the embedding potential $u_{emb}(\vec{r},t)$ as an additional external potential, while treating $A_{\rm int}$ with proper approximations. If the exact $A_{\rm int}$, formally defined in Eq. (6), is employed, we just recover the total action A_{tot} and no computational cost will be saved. Technically, the major task in TD-PFET is to obtain $u_{emb}(\vec{r},t)$ by solving Eq. (8), which is numerically very challenging. We now discuss some ways to simplify Eq. (8) to make it easily solvable.

We proceed by inserting the identity Eq. (3) into Eq. (8), and obtain

$$\sum_K \frac{\delta A_K}{\delta u_{emb}(\vec{r},t)} + \frac{\delta A_{tot}}{\delta u_{emb}(\vec{r},t)} - \sum_K \frac{\delta A_K}{\delta u_{emb}(\vec{r},t)} = i\left\langle \Psi_{tot,T}\left| \frac{\delta \Psi_{tot,T}}{\delta u_{emb}(\vec{r},t)}\right\rangle. \tag{13}$$

By the chain rule, the third term on the LHS of Eq. (13) can be written as

$$\frac{\delta A_K}{\delta u_{emb}(\vec{r},t)} \equiv \iint d\vec{r}'dt' \left.\frac{\delta A_K}{\delta \rho_K(\vec{r}',t')}\right|_{u_{emb}} \frac{\delta \rho_K(\vec{r}',t')}{\delta u_{emb}(\vec{r},t)} - \rho_K,$$

where A_K is treated as a functional of both u_{emb} and ρ_K (ρ_K is also a functional of u_{emb}). The first term on the LHS of Eq. (13) can be replaced by the identity Eq. (12), therefore Eq. (13) becomes

$$\iint d\vec{r}'dt' \sum_K \left.\frac{\delta(A_{tot}-A_K)}{\delta \rho_K(\vec{r}',t')}\right|_{u_{emb}} \frac{\delta \rho_K(\vec{r}',t')}{\delta u_{emb}(\vec{r},t)} - \Delta B = 0, \tag{14}$$

where we have exploited the fact that A_{tot} does not explicitly depend on $u_{emb}(\vec{r},t)$. ΔB is defined as

$$\Delta B = i\left\langle \Psi_{tot,T}[u_{emb}]\left| \frac{\delta \Psi_{tot,T}[u_{emb}]}{\delta u_{emb}(\vec{r},t)}\right\rangle - \sum_K i\left\langle \Psi_{K,T}[u_{emb}]\left| \frac{\delta \Psi_{K,T}[u_{emb}]}{\delta u_{emb}(\vec{r},t)}\right\rangle. \right. \tag{15}$$

The reason that we treat the first and the second $\sum_K \delta A_K/\delta u_{emb}$ terms in Eq. (13) differently will be explained later.

Until this point no approximation has been made and Eq. (14) is formally exact. Any approximation made to Eq. (14) will affect the exactness of $u_{emb}(\vec{r},t)$, which in turn will affect the time evolution of subsystems, as well as the total system.

It is very challenging to evaluate ΔB, as it depends on the boundary terms from both the total system and subsystems. The second boundary term, due to subsystems, on the right hand side (RHS) of Eq. (15), can be removed if subsystems are propagated by TDDFT methods that ignore causality, such as TDDFT using ALDA.[58,59] If we also set the first boundary term on the RHS of Eq. (15) to zero, i.e., we ignore the causality of the total system, we reach $\Delta B = 0$. One may ask whether it is physical to ignore causality in the total system and the subsystems. We argue that even if each boundary term on the RHS of Eq. (15) is nonzero, we might still be able to approximate $\Delta B = 0$ in practice. To justify this argument, note that ΔB can be treated as a special interaction term resulting from boundary conditions. If the absolute values of these boundary terms are much smaller than other terms, e.g., the Hartree or XC term, we expect that the final electron dynamics would not change much by setting $\Delta B = 0$. However, such an argument should be verified numerically in future TD-PFET simulations.

To find possible ways to approximate the integral on the LHS of Eq. (14), we re-write the actions in the time-dependent Kohn-Sham style,[6]

$$A = S_0 - A_{XC} - A_H - \iint d\vec{r}dt\,\rho(\vec{r},t)v(\vec{r},t),$$

where $v(\vec{r},t)$ is the time-dependent external potential, the Hartree term A_H is $\iint d\vec{r}d\vec{r}'\frac{\rho(\vec{r},t)\rho(\vec{r}',t)}{|\vec{r}-\vec{r}'|}$, and S_0 is defined as

$$S_0 = \int_0^T \sum_j \langle \phi_j(t)|i\partial_t + \frac{1}{2}\nabla^2|\phi_j(t)\rangle dt, \tag{16}$$

with $\{\phi_j(t)\}$ being the time-dependent Kohn-Sham orbitals. A_{XC} is the XC action, i.e., between A and $[S_0 - A_H - \iint d\vec{r}dt\,\rho(\vec{r},t)v(\vec{r},t)]$.

By inserting the above expression for A into Eq. (14), we obtain

$$\left.\frac{\delta(A_{tot}-A_K)}{\delta \rho_K(\vec{r},t)}\right|_{u_{emb}} = \frac{\delta(S_{tot,0}-S_{K,0})}{\delta \rho_K(\vec{r},t)} - \frac{\delta}{\delta \rho_K(\vec{r},t)}\left(A_{XC}\left[\sum_K \rho_K\right] - A_{XC}[\rho_K]\right)$$

This article is copyrighted as indicated in the article. Reuse of AIP content is subject to the terms at: http://scitation.aip.org/termsconditions. Downloaded to IP: 66.67.101.221 On: Mon, 31 Mar 2014 14:59:43

$$-\frac{\delta}{\delta\rho_K(\vec{r},t)}\left(A_H\left[\sum_K \rho_K\right]-A_H[\rho_K]\right)$$
$$-(v_{ion,tot}(\vec{r})-v_{ion,K}(\vec{r})-u_{emb}(\vec{r},t)), \quad (17)$$

where $v_{ion,tot}$ and $v_{ion,K}$ are respectively the ionic potentials of the total system and subsystem K.

Equation (17) provides us a way to further approximate the integral equation (14) by evaluating A_K using approximate functionals. This is the reason that we treat the two $\sum_K \delta A_K/\delta u_{emb}$ terms in Eq. (13) differently. The first $\sum_K \delta A_K/\delta u_{emb}$ term in Eq. (13) is treated exactly (using the identity Eq. (12)), and the second $\sum_K \delta A_K/\delta u_{emb}$ term in Eq. (13) will be treated approximately in what follows.

In practice, approximate functionals such as the ALDA might be used for the A_{XC} in Eq. (17); i.e., the embedding potential would be evaluated on the ALDA level while the time propagation of each subsystem is handled by a higher-level method. This results in a similar framework as for our previous time-independent embedding calculations,[20,28] where the LDA or generalized gradient approximations were used for evaluating the XC functionals in the interaction term. If we were to ignore the terms containing $S_{tot,0}$ and $S_{K,0}$ in Eq. (17), the interaction between subsystems would only be due to the Coulomb and XC parts. If we were to further discard the XC terms in Eq. (17), the embedding would then be purely based on electrodynamics.

According to Ref. 58, the functional derivative of S_0 with respect to $\rho(\vec{r},t)$ is

$$\frac{\delta S_0}{\delta\rho(\vec{r},t)}=v_{eff}(\vec{r},t)+\sum_j i\left\langle\phi_{jT}\left|\frac{\delta\phi_{jT}}{\delta\rho(\vec{r},t)}\right\rangle\right., \quad (18)$$

where $v_{eff}(\vec{r},t)$ is the time-dependent Kohn-Sham effective potential that drives $\{\phi_j(\vec{r},t)\}$ as $i\partial_t\phi_j(\vec{r},t)=(-\frac{1}{2}\nabla^2+v_{eff}(\vec{r},t))\phi_j(\vec{r},t)$, and ϕ_{jT} stands for $\phi_j(\vec{r},t=T)$. In Eq. (18), boundary terms again arise due to the time-dependent Kohn-Sham orbitals $\phi_j(\vec{r},t=T)$.

Using Eq. (18), we have for the first term on the RHS of Eq. (17),

$$\frac{\delta(S_{tot,0}-S_{K,0})}{\delta\rho_K(\vec{r},t)}$$
$$=\left(v_{eff}\left[\sum_K\rho_K\right](\vec{r},t)-v_{eff}[\rho_K](\vec{r},t)\right)$$
$$+\left[\sum_j i\left\langle\phi_{tot,jT}\left|\frac{\delta\phi_{tot,jT}}{\delta\rho_K(\vec{r},t)}\right\rangle\right.\right.$$
$$\left.\left.-\sum_j i\left\langle\phi_{K,jT}\left|\frac{\delta\phi_{K,jT}}{\delta\rho_K(\vec{r},t)}\right\rangle\right.\right], \quad (19)$$

where troublesome boundary terms that include $\phi_{tot,jT}$ and $\phi_{K,jT}$ again plague the evaluation of Eq. (19). If we again neglect causality,[58] these boundary terms can be removed. The only terms left in Eq. (19) contain v_{eff}, which can be evaluated for a given v-representative time-dependent electron density as discussed in Sec. II D.

C. TDDFT/ALDA-in-TDDFT/ALDA embedding

After demonstrating some ways to simplify Eq. (8), as proof-of-principle we now show how to simplify TDPFET for a more straightforward case: TDDFT/ALDA-in-TDDFT/ALDA embedding, in which the XC functionals in Eq. (17) are approximated by ALDA and all subsystems are propagated using TDDFT/ALDA. No boundary term appears in the formalism of TDDFT/ALDA.[58] Therefore, Eq. (13) can be greatly simplified for TDDFT/ALDA-in-TDDFT/ALDA embedding by removing all the boundary terms. We finally have

$$\sum_K\iint d\vec{r}'dt'\left[\left.\frac{\delta A_K}{\delta\rho_K(\vec{r}',t')}\right|_{u_{emb}}\right.$$
$$\left.+\left(\frac{\delta A_{tot}}{\delta\rho_K(\vec{r}',t')}-\left.\frac{\delta A_K}{\delta\rho_K(\vec{r}',t')}\right|_{u_{emb}}\right)\right]\frac{\delta\rho_K(\vec{r}',t')}{\delta u_{emb}(\vec{r},t)}=0. \quad (20)$$

In Eq. (20) ρ_K is evaluated for any given u_{emb}, and the total electron density is obtained as $\rho_{tot}=\sum_K\rho_K$. As written, the terms inside the square bracket on the LHS of Eq. (20) imply that for subsystem K there is an additional time-dependent external potential,

$$v_{add,K}(\vec{r},t)=\frac{\delta A_{tot}}{\delta\rho_K(\vec{r},t)}-\left.\frac{\delta A_K}{\delta\rho_K(\vec{r},t)}\right|_{u_{emb}}.$$

Since no boundary term appears in the formalism of TDDFT/ALDA, we have $\frac{\delta A_K}{\delta\rho_K}|_{u_{emb}}=0$. By the chain rule, $\frac{\delta A_{tot}}{\delta\rho_K}$ is just equal to $\frac{\delta A_{tot}}{\delta\rho_{tot}}$. Therefore $v_{add,K}$ does not depend on K. To iteratively solve for $u_{emb}(\vec{r},t)$ we simply update it as

$$u^{(n+1)}_{emb,K}(\vec{r},t)=u^{(n)}_{emb,K}(\vec{r},t)-v_{add,K}(\vec{r},t)$$
$$=u^{(n)}_{emb,K}(\vec{r},t)-\frac{\delta A_{tot}}{\delta\rho_{tot}(\vec{r},t)}, \quad (21)$$

with n being the iteration number. Equation (21) also ensures that we always have a common time-dependent embedding potential for all subsystems. The $\delta A_{tot}/\delta\rho_{tot}$ term in Eq. (21) can be decomposed as

$$\frac{\delta A_{tot}}{\delta\rho_{tot}}=v_{eff}[\rho_{tot}]-v_{XC}[\rho_{tot}]-v_H[\rho_{tot}]-v_{ion,tot}-v_{td}, \quad (22)$$

where $v_{eff}[\rho_{tot}]$ is the time-dependent Kohn-Sham effective potential associated with density $\rho_{tot}(\vec{r},t)$ [we discuss in detail how to solve for $v_{eff}[\rho_{tot}]$ in Sec. II D], the XC potential is $v_{XC}=\frac{\delta A^{ALDA}_{XC}[\rho_{tot}]}{\delta\rho_{tot}}$, v_H is the Hartree potential, $v_{ion,tot}(\vec{r})$ is the ionic potential of the total system, and $v_{td}(\vec{r},t)$ is the time-dependent external potential, e.g., time-dependent laser field. When Eq. (21) converges, we reach $\frac{\delta A_{tot}}{\delta\rho_{tot}}=0$ which makes Eq. (20) hold. Technically we just need to solve the coupled Eqs. (21) and (22), which is discussed in detail in Sec. III.

D. Inversion of the time-dependent Kohn-Sham equation for a *v*-representable electron density

We now focus on how to obtain the $v_{eff}(\vec{r},t)$ in Eq. (22) for a given time-dependent electron density. Unlike our earlier

This article is copyrighted as indicated in the article. Reuse of AIP content is subject to the terms at: http://scitation.aip.org/termsconditions. Downloaded to IP: 66.67.101.221 On: Mon, 31 Mar 2014 14:59:43

time-independent potential functional embedding formulation in which we could use the Wu-Yang inversion method,[60] here we cannot do so because in principle $\frac{\delta A}{\delta v_{eff}(\vec{r},t)}$ is nonzero. Even if for the TDDFT/ALDA case $\frac{\delta A}{\delta v_{eff}(\vec{r},t)}$is zero due to the vanishing of boundary terms as discussed above, we still cannot solve for $v_{eff}(\vec{r},t)$ by minimizing the action A with respect to $v_{eff}(\vec{r},t)$ as suggested in Ref. 60, since the solution is the stationary point of action A.

Instead, we extend the Zhao-Morrison-Parr (ZMP) method,[61] originally introduced for time-independent quantum systems, to time-dependent quantum systems. Our time-dependent version of the ZMP method is denoted as "TDZMP" in what follows. Here, the penalty functional in the original ZMP method[61] is modified to

$$V_{\text{penalty}}[\rho] = \frac{\lambda}{2}\int dt \iint d\vec{r}d\vec{r}' \times \frac{(\rho(\vec{r},t)-\rho_{\text{ref}}(\vec{r},t))(\rho(\vec{r}',t)-\rho_{\text{ref}}(\vec{r}',t))}{|\vec{r}-\vec{r}'|},$$

where $\rho_{\text{ref}}(\vec{r},t)$ is the target time-dependent electron density.

The time-dependent Kohn-Sham equations in TDZMP are

$$i\partial_t\phi_j(\vec{r},t) = \left[-\frac{1}{2}\nabla^2 + v_{eff,\text{approx}}[\rho](\vec{r},t) + v_{\text{penalty}}[\rho](\vec{r},t)\right] \times \phi_j(\vec{r},t), \quad (23)$$

where $\rho(\vec{r},t)=\sum_j|\phi_j(\vec{r},t)|^2$ and $v_{eff,\text{approx}}$ is an approximated time-dependent Kohn-Sham effective potential. The potential $v_{\text{penalty}}[\rho]$, due to $V_{\text{penalty}}[\rho]$, is

$$v_{\text{penalty}}(\vec{r},t) = \lambda\int d^3r'\frac{\rho(\vec{r}',t)-\rho_{\text{ref}}(\vec{r}',t)}{|\vec{r}-\vec{r}'|}. \quad (24)$$

For a given λ, the coupled Eqs. (23) and (24) are solved self-consistently. The resulting time-dependent Kohn-Sham effective potential for this λ is

$$v_{eff,\lambda}(\vec{r},t) = v_{eff,\text{approx}}[\rho](\vec{r},t) + v_{\text{penalty}}[\rho](\vec{r},t).$$

To accelerate convergence when solving the coupled Eqs. (23) and (24), one needs to construct a $v_{eff,\text{approx}}$ that is close to $v_{eff,\lambda}(\vec{r},t)$. In this work, $v_{eff,\text{approx}}$ consists of the time-dependent external potential (the laser field), the ionic potential, and the Hartree potential (evaluated based on $\rho_{\text{ref}}(\vec{r},t)$). Since the time-dependent XC potential for $\rho_{\text{ref}}(\vec{r},t)$ is not known, we do not add it to $v_{eff,\text{approx}}$.

To obtain the exact time-dependent Kohn-Sham effective potential, i.e., $v_{eff,\lambda=\infty}(\vec{r},t)$, one can extrapolate to it by solving Eqs. (23) and (24) for several different λs.

III. NUMERICAL DETAILS

In all calculations, a plane wave basis kinetic energy cutoff of 600 eV, Fermi-Dirac smearing with a smearing width of 0.1 eV, and the Perdew-Wang LDA[62] XC functional were used. The geometry of the Na_4 cluster was taken from our previous work,[63] in which the cluster atoms lie in the x-y plane (Fig. 1(b)). The distance between Na_{top} and Na_{bottom} is 6.51 Å, and between Na_{left} and Na_{right} is 3.05 Å. The Na_4 cluster was placed in vacuum within a periodic cell of 15 × 15 × 15 Å. The norm-conserving pseudopotential for Na was generated using the FHI98 code[64] with its default cutoff radii.

Before performing TD-PFET calculations, a PFET[35] calculation was carried out, where each Na atom was treated as one subsystem. The PFET results were then used as input for the following TD-PFET calculations. PFET is implemented in the ABINIT[65] code; details can be found in Ref. 35. All TDDFT and TDZMP calculations were performed using a homemade code implemented in ABINIT. To perform TD-PFET, a custom FORTRAN90 code drives both the TDDFT and TDZMP codes.

We obtain the time-independent embedding potential $u_{emb}^{\text{PFET}}(\vec{r})$ with PFET. The subsystem electron numbers optimize to 1.057 and 0.943 for Na_{top} (and Na_{bottom}) and Na_{right} (and Na_{left}), respectively, where the fractional electron numbers result from the equilibration of chemical potentials among the subsystems.[35] The total electron density $\rho_{tot}^{\text{PFET}}(\vec{r})$ is then obtained by superposing all subsystem electron densities. The Kohn-Sham orbitals $\{\phi_{i,tot}^{\text{PFET}}(\vec{r})\}$ and the Kohn-Sham effective potential $v_{eff,tot}^{\text{PFET}}(\vec{r})$ associated with $\rho_{tot}^{\text{PFET}}(\vec{r})$ are obtained by performing the Wu-Yang optimized effective potential scheme,[60] with a regularization coefficient[66] of 1×10^{-8}. The sum of XC and Hartree potentials is obtained as $v_{\text{HXC}}^{\text{PFET}}(\vec{r}) = v_{eff,tot}^{\text{PFET}}(\vec{r}) - v_{ion,tot}(\vec{r})$. Then, $u_{emb}^{\text{PFET}}(\vec{r})$, $v_{\text{HXC}}^{\text{PFET}}(\vec{r})$, $\rho_{tot}^{\text{PFET}}(\vec{r})$, and $\{\phi_{i,tot}^{\text{PFET}}(\vec{r})\}$ are supplied for TD-PFET calculations.

The steps for performing TD-PFET are

1. Propagate each subsystem using TDDFT/ALDA from t to $t+\Delta t$, with the trial $u_{emb}(\vec{r},t)$ as an additional external potential. At $t=0$, $u_{emb}(\vec{r},t)$ is taken as $u_{emb}^{\text{PFET}}(\vec{r})$.
2. Obtain the total electron density $\rho_{tot}(\vec{r},t+\Delta t)$ by superposing all subsystem electron densities $\{\rho_K(\vec{r},t+\Delta t)\}$.
3. The $v_{eff}(\vec{r},t+\Delta t)$ and $\{\phi_{i,tot}(\vec{r},t+\Delta t)\}$ associated with $\rho_{tot}(\vec{r},t+\Delta t)$ are obtained using TDZMP. To perform TDZMP, v_{eff} and $\{\phi_{i,tot}\}$ from the previous time step are needed. At the first time step, $v_{\text{HXC}}^{\text{PFET}}(\vec{r})$ and $\{\phi_{i,tot}^{\text{PFET}}(\vec{r})\}$ from the PFET calculations are used.
4. With $v_{eff}(\vec{r},t+\Delta t)$ and $\rho_{tot}(\vec{r},t+\Delta t)$ in hand, we evaluate $\frac{\delta A_{tot}}{\delta\rho_K}$ with Eq. (22) and then update $u_{emb}(\vec{r},t+\Delta t)$ with Eq. (21).
5. If $\rho_{tot}(\vec{r},t+\Delta t)$ is not converged, we return to step 1.

Once the above cycle for evaluating $u_{emb}(\vec{r},t+\Delta t)$ is finished, we move on to solve for $u_{emb}(\vec{r},t+2\Delta t)$.

In this work, a laser pulse is applied in the y direction (Fig. 1(b)). Its electric part is $\vec{E}=\Re[A\exp(i\omega t)]\hat{y}$, with the envelope defined as $A=a_0\cos(\pi(t-2\tau_0-t_0)/2\tau_0)$. Parameters used are $\tau_0=0.2$ fs, $t_0=0.2$ fs, $\omega=18$ fs^{-1}, and $a_0=2.0$ V/Å. The laser is turned off (set to zero) after $t=0.4$ fs. A time step of 0.01 fs was found small enough to converge the electron dynamics.

Usually, time-dependent Kohn-Sham equations are propagated using the second-order Crank-Nicolson scheme,[67,68]

$$\phi_j(\vec{r},t+\Delta t) = \frac{\left(1-\frac{i}{2}\left(\frac{H(t+\Delta t)+H(t)}{2}\right)\Delta t\right)}{\left(1+\frac{i}{2}\left(\frac{H(t+\Delta t)+H(t)}{2}\right)\Delta t\right)}\phi_j(\vec{r},t), \quad (25)$$

This article is copyrighted as indicated in the article. Reuse of AIP content is subject to the terms at: http://scitation.aip.org/termsconditions. Downloaded to IP: 66.67.101.221 On: Mon, 31 Mar 2014 14:59:43

where $H(t)$ is the Kohn-Sham Hamiltonian at time t. Using the above propagator, the amplitude of $u_{emb}(\vec{r}, t)$ increases dramatically over time in our TD-PFET simulations. To avoid this instability, we suppress the transfer of numerical errors from time t to $t + \Delta t$ by using instead the first-order Crank-Nicolson propagator,

$$\phi_j(\vec{r}, t + \Delta t) = \frac{\left(1 - \frac{i}{2}H(t + \Delta t)\Delta t\right)}{\left(1 + \frac{i}{2}H(t + \Delta t)\Delta t\right)}\phi_j(\vec{r}, t). \quad (26)$$

The above propagator [Eq. (26)] only depends on $H(t + \Delta t)$, therefore $u_{emb}(\vec{r}, t + \Delta t)$ no longer needs to compensate for any numerical error in $u_{emb}(\vec{r}, t)$, which greatly suppresses the transfer of numerical error from $u_{emb}(\vec{r}, t)$ to $u_{emb}(\vec{r}, t + \Delta t)$. By contrast, the second-order Crank-Nicolson propagator [Eq. (25)] is determined by $\frac{1}{2}(u_{emb}(\vec{r}, t + \Delta t) + u_{emb}(\vec{r}, t))$, and any numerical error in $u_{emb}(\vec{r}, t)$ will be transferred to and accumulate in $u_{emb}(\vec{r}, t + \Delta t)$.

The first-order propagator [Eq. (26)] also stabilizes the TDZMP calculations. In TDZMP, $H(t + \Delta t)$ is just $-\frac{1}{2}\nabla^2 + v_{eff,\lambda}(\vec{r}, t + \Delta t)$, where $v_{eff,\lambda}(\vec{r}, t + \Delta t)$ is what we are solving for. $\phi_j(\vec{r}, t + \Delta t)$ in Eq. (26) is then solely determined by $v_{eff,\lambda}(\vec{r}, t + \Delta t)$ and $\phi_j(\vec{r}, t)$, instead of $\frac{1}{2}(v_{eff,\lambda}(\vec{r}, t + \Delta t) + v_{eff,\lambda}(\vec{r}, t))$ as in the case of using the second-order Crank-Nicolson propagator [Eq. (25)]. In this way, we again greatly suppress the transfer of any numerical error from $v_{eff,\lambda}(\vec{r}, t)$ to $v_{eff,\lambda}(\vec{r}, t + \Delta t)$.

IV. RESULTS AND DISCUSSION

We demonstrate TD-PFET on a Na_4 cluster subject to an external laser field as described in Sec. III. The laser is turned on at $t = 0$ and then turned off (set to zero) after 0.4 fs [see Fig. 2(c)]. TDDFT/ALDA calculations on the entire (i.e., non-embedded) Na_4 cluster provide our benchmark [black solid lines in Figs. 2(a) and 2(b)].

We show the time evolution of the electric dipoles from TD-PFET calculations [Fig. 2(a)] for three different penalty-function coefficients: $\lambda = 2 \times 10^4$ (red dotted line), $\lambda = 7 \times 10^3$(green dotted-dashed line), and $\lambda = 2 \times 10^3$ (orange dotted-dotted-dashed line). The electric dipole for infinitely large λ is extrapolated (blue dashed line) from them. As expected, larger λ gives a curve closer to the benchmark. The small residual difference between the benchmark and the extrapolated curve is attributed to the numerical errors in our implementation of TD-PFET. Note that although the deviations between the benchmark and the extrapolated curves slowly increase with time, they do not obscure subtle features in the dipole evolution: for large t after the pulse, the benchmark predicts residual oscillations in the electric dipole [black arrows in Fig. 2(a)]. The positions and magnitudes of these small oscillations are all correctly reproduced by TD-PFET. For comparison, we also perform a TD-PFET calculation by fixing $u_{emb}(\vec{r}, t)$ to $u_{emb}^{\mathrm{PFET}}(\vec{r})$ at all time. The result (purple circles) differs significantly from the benchmark, which indicates that we cannot simply replace the time-dependent embedding potential with the embedding potential from a time-independent embedding calculation. A true TD-PFET simulation is essential.

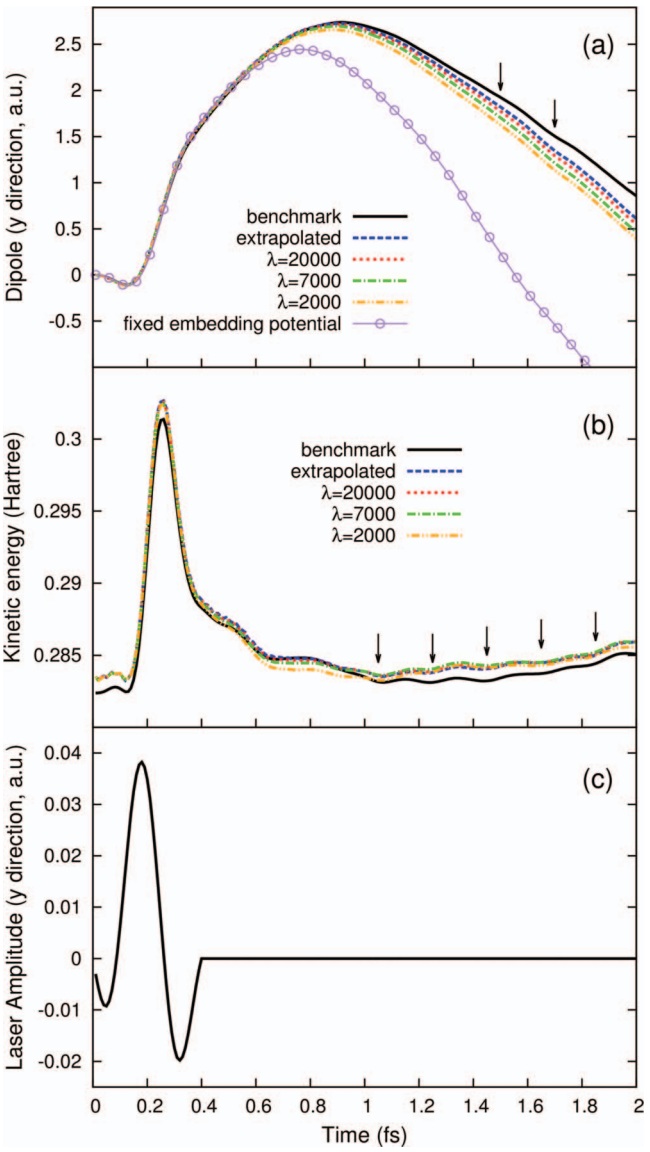

FIG. 2. Time evolution of a Na_4 cluster in a laser field, as predicted by TD-PFET compared to full TDDFT benchmark calculations. (a) Comparison of electric dipoles in the y direction. The purple circles are obtained by fixing $u_{emb}(\vec{r}, t)$ to $u_{emb}^{\mathrm{PFET}}(\vec{r})$ during the TD-PFET simulation. (b) Comparison of the non-interacting Kohn-Sham kinetic energies. (c) Amplitude of the applied laser, in the y direction. All axes are in atomic units. In (a) and (b), the full-system benchmarks are shown as black solid curves, results from TD-PFET simulations with penalty coefficients $\lambda = 20\,000$, $\lambda = 7000$, and $\lambda = 2000$ as red dotted, green dotted-dashed, and orange dotted-dotted-dashed curves, respectively. The $\lambda = \infty$ curve (blue dashed curves) are extrapolated from these three TD-PFET curves. In (a) and (b), TD-PFET correctly reproduces the small oscillations (marked with arrows) of the benchmark.

We also compare the time-dependent kinetic energy $\tau(t)$ [see Fig. 2(b)], defined as

$$\tau(t) = \sum_{i=occ} \int dr^3 \phi_i^*(\vec{r}, t)\left(-\frac{1}{2}\nabla^2\right)\phi_i(\vec{r}, t),$$

where $\phi_i(\vec{r}, t)$ is the ith complex time-dependent Kohn-Sham orbital obtained via inversion of the time-dependent total electron density (superposition of time-dependent subsystem electron densities) using the TDZMP method. For an isolated system, $\tau(t)$ is real. TD-PFET reproduces the benchmark very

This article is copyrighted as indicated in the article. Reuse of AIP content is subject to the terms at: http://scitation.aip.org/termsconditions. Downloaded to IP: 66.67.101.221 On: Mon, 31 Mar 2014 14:59:43

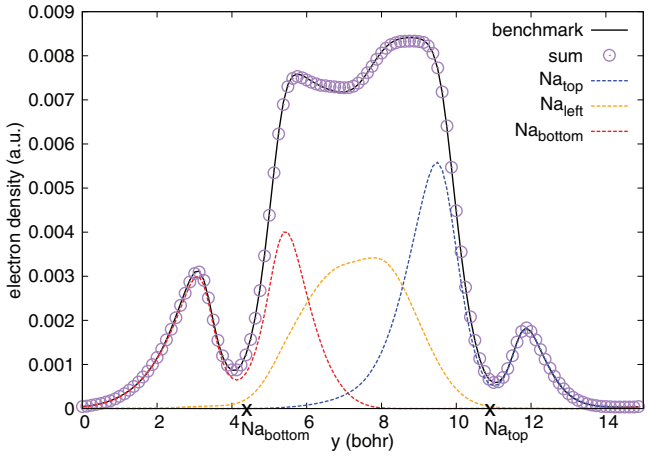

FIG. 3. Snapshot of Na_4 electron density profiles (in atomic units) at $t = 1.0$ fs between Na_{top} and Na_{bottom} (along the dashed line in Fig. 1(b)). The full-system benchmark is shown as the black solid curve, with the density profiles of the four Na atoms (subsystems) shown as dashed lines. The sum of subsystem electron densities is in purple circles, which matches the benchmark very well. Due to the symmetry of the cluster, the electron densities from Na_{left} and Na_{right} are almost identical; we thus only show Na_{left}. The positions of Na_{top} and Na_{bottom} are marked by "X"s. We find that the electron densities are polarized towards Na_{top}.

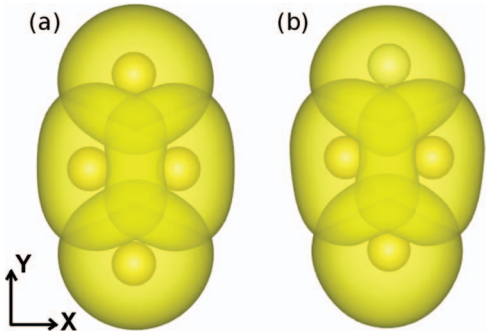

FIG. 4. Superpositions of four subsystem electron densities (isosurface is 6×10^{-4} 1/bohr^3 for all subsystems) at $t = 0$ fs (a) and $t = 1.0$ fs (b). Yellow balls indicate Na nuclei. At $t = 1.0$ fs, all subsystems are polarized in the laser direction (y direction).

well [Fig. 2(b)]. Once again, the TD-PFET results with larger penalty function coefficients are closer to the benchmark. At $t = 0$ fs, we find a 1.1 mHa difference in kinetic energy between the benchmark and TD-PFET. This is due to the fact that $\rho_{tot}^{\mathrm{PFET}}(\vec{r})$ is slightly different from the ground state electron density obtained by performing Kohn-Sham DFT/LDA on the whole Na_4 cluster. Therefore the kinetic energy $\tau(t = 0)$ inverted from $\rho_{tot}^{\mathrm{PFET}}(\vec{r})$ is slightly different from the benchmark. Nevertheless, TD-PFET accurately reproduces the peak of $\tau(t)$ at 0.26 fs, as well as the many small oscillations marked by black arrows.

We further assess the quality of TD-PFET by comparing the electron density profiles (Fig. 3) at $t = 1.0$ fs. The sum of subsystem electron densities (purple circles) matches the benchmark (black solid curve) very well. We observe that, as expected from the direction of the electric field, the electron density is polarized towards Na_{top}.

In addition to reproducing the time-dependent behavior of the full system, TD-PFET allows us to study the time evolution of subsystems. At $t = 0$ fs, the electric dipole moment of the Na_4 cluster is zero, as confirmed by the symmetric electron densities between Na_{top} and Na_{bottom}, and between Na_{left} and Na_{right} [see Fig. 4(a)]. At $t = 1.0$ fs, the electron densities of all Na atoms are polarized by the laser in the y direction [see Fig. 4(b)] to produce a net electric dipole.

V. COMPARISON TO THE "FRAGMENT-TIME-DEPENDENT DENSITY FUNCTIONAL THEORY"

During the preparation of this paper, we became aware of a related work by Wasserman *et al.*,[69] which introduced a fragment-based time-dependent density functional theory to solve large time-dependent systems in a divide-and-conquer manner. They provide a differential equation that relates the global partitioning potential (which resembles our embedding potential) to the total density evolution [see Eq. (19) in Ref. 69], which can be used to propagate the partitioning potential. However, the resulting propagation scheme relies on an independent propagation of the total electron density. To better understand this point, we re-derive their Eq. (19). Starting from the continuity equation for subsystem α, we obtain

$$\begin{aligned}\frac{\partial^2 n_\alpha(\vec{r},t)}{\partial t^2} &= i\nabla\cdot\mathrm{Tr}\{\hat{\Gamma}_{s,\alpha}[\hat{\mathbf{j}}(t),\hat{H}_{s,\alpha}(t)]\}\\ &= i\nabla\cdot\mathrm{Tr}\{\hat{\Gamma}_{s,\alpha}[\hat{\mathbf{j}}(t),\hat{T}_s(t)]\}\\ &\quad + i\nabla\cdot\mathrm{Tr}\{\hat{\Gamma}_{s,\alpha}[\hat{\mathbf{j}}(t),v_p+v_{Hxc}+v_\alpha]\}\\ &= i\nabla\cdot\mathrm{Tr}\{\hat{\Gamma}_{s,\alpha}[\hat{\mathbf{j}}(t),\hat{T}_s(t)]\}\\ &\quad + \nabla\cdot[n_\alpha\nabla v_p]+\nabla\cdot[n_\alpha\nabla(v_{Hxc}+v_\alpha)], \quad (27)\end{aligned}$$

where the same notations as in Ref. 69 are used. [Note the unconventional sign of the probability current below Eq. (4) in Ref. 6 would give an opposite sign for the potential terms, the last two terms, in Eq. (27).]. $n_\alpha(\vec{r},t)$ is the electron density of subsystem α, $\hat{\Gamma}_{s,\alpha}$ is the density matrix of subsystem α, $\hat{\mathbf{j}}$ is the probability current operator, $v_p(\vec{r},t)$ is the time-dependent partition potential (denoted as the embedding potential in our work), and $v_\alpha(\vec{r})$ is the ionic potential of subsystem α. After summing up the above equation for all subsystems, we reach Eq. (19) in Ref. 69. Since Eq. (27) follows from the continuity equation for each subsystem, it holds for any given embedding potential $v_p(\vec{r},t)$. Hence Eq. (19) in Ref. 69 holds for any $v_p(\vec{r},t)$, as long as the total electron density is obtained by $n(\vec{r},t)=\sum_\alpha n_\alpha(\vec{r},t)$. Consequently, one requires a different approach to *first* determine the total time-dependent electron density $n(\vec{r},t)$, before solving for the partitioning potential using Eq. (19) in Ref. 69.

By contrast, our scheme does not require an independent calculation of $n(\vec{r},t)$: a general integral equation Eq. (8) for solving for the time-dependent embedding potential is derived in this work based on the action of time-dependent quantum mechanics. The quality of the embedding is then determined by the level of approximations used for solving Eq. (8). Finally, our framework also allows for using different levels of theory in different subsystems.

This article is copyrighted as indicated in the article. Reuse of AIP content is subject to the terms at: http://scitation.aip.org/termsconditions. Downloaded to IP: 66.67.101.221 On: Mon, 31 Mar 2014 14:59:43

VI. CONCLUSIONS

We introduced a time-dependent potential-functional embedding theory, which offers the possibility to simulate different regions in molecules or materials with different time-dependent quantum mechanics methods endowed with different levels of accuracy. By constraining all subsystems to share a common time-dependent embedding potential, the embedding potential is proved to be unique (up to an undetermined time-dependent constant, see the Appendix) for a given time-dependent quantum system, which makes our TD-PFET tractable for practical use. We derived an integral equation to solve for this unique time-dependent embedding potential and discussed practical means to approximately solve it. For the straightforward case of TDDFT/ALDA-in-TDDFT/ALDA embedding, we showed how to solve for the embedding potential using a simple iterative scheme, and demonstrated it for a Na_4 cluster, in which each Na atom was treated as a subsystem.

Our Na_4 cluster test demonstrated that the TDZMP method is quite time-consuming. Therefore it would be desirable to find an alternative approach to evaluate more quickly the time-dependent Kohn-Sham effective potential for a given time-dependent electron density. One promising approach is the recently introduced time-dependent orbital-free density functional theory (TD-OFDFT),[70] in which the time-dependent Kohn-Sham effective potential is approximated without invoking time-dependent Kohn-Sham orbitals. TD-PFET would greatly benefit from further developments of TD-OFDFT, whose efficiency and accuracy was recently demonstrated for free-electron-like systems.[70]

Future work could apply TD-PFET to study materials in which a region of interest would be best described by more accurate but more expensive time-dependent quantum mechanics methods, such as TDCW methods or TDDFT equipped with advanced orbital-dependent time-dependent XC functionals,[71–73] while the environment could be treated efficiently by low-level time-dependent quantum mechanics methods, e.g., TDDFT/ALDA. Numerical challenges in solving the nonlinear Eq. (8) must be overcome for such advanced applications. Ultimately, we hope TD-PFET will prove useful for studying electron dynamics in materials and biomolecules, where characterization of electronic motion is often crucial to understanding their properties (e.g., in photovoltaics and photosynthetic reaction centers). We anticipate applications of our theory to include surface-enhanced Raman spectroscopy, spectra of dye molecules in dye-sensitized solar cells. By treating the electron donor and acceptor together as one subsystem, while the surrounding environment is handled with a cheaper method, our TD-PFET might be found useful to study charge transfer and separation in light-harvesting molecules and materials.

ACKNOWLEDGMENTS

Some of the calculations were performed on the TIGRESS high-performance computing cluster at Princeton University. We thank Dr. Kieron Burke for discussions on TDDFT, and Dr. Adam Wasserman and Martin Mosquera for pointing out the unconventional definition of probability current in Ref. 6. F.L. acknowledges support by the SFB VICOM (SFB-041 ViCoM), funded by the FWF, and E.A.C. thanks the National Science Foundation (CHE-1265700) for support of this work.

APPENDIX: PROOF OF THE UNIQUENESS OF THE TIME-DEPENDENT EMBEDDING POTENTIAL

We show in the following that once a time-dependent quantum system is selected and the grouping of atoms is done, $u_{emb}(\vec{r}, t)$ is uniquely determined up to a time-dependent constant $c(t)$. Our proof for such uniqueness is an extension of the Runge-Gross theorem.

Suppose that at $t = 0$, the system is in its ground state with its time-independent embedding potential $u_{emb}(\vec{r}, 0)$, which is unique and can be obtained from PFET.[35] At $t > 0$, let us assume that $u_{emb}(\vec{r}, 0)$ evolves into two different time-dependent embedding potentials $u_{emb}(\vec{r}, t)$ and $u'_{emb}(\vec{r}, t)$ that yield the same time-dependent total electron density, i.e., $\rho_{tot}(\vec{r}, t) = \sum_K \rho_K(\vec{r}, t) = \sum_K \rho'_K(\vec{r}, t)$. We now prove that $u_{emb}(\vec{r}, t)$ and $u'_{emb}(\vec{r}, t)$ can only differ by a time-dependent constant, which means that if we expand $u_{emb}(\vec{r}, t)$ and $u'_{emb}(\vec{r}, t)$ in a Taylor series around $t = 0$, we should have for all orders l,

$$\frac{\partial^l}{\partial t^l}(u_{emb}(\vec{r}, t) - u'_{emb}(\vec{r}, t))|_{t=0} = \text{const.} \tag{A1}$$

Our proof for Eq. (A1) proceeds by *reductio ad absurdum*: we assume that $u_{emb}(\vec{r}, t)$ and $u'_{emb}(\vec{r}, t)$ differ at some point $t > 0$. Then their Taylor expansion at $t = 0$ must already differ at some finite order l

$$\frac{\partial^l}{\partial t^l}(u_{emb}(\vec{r}, t) - u'_{emb}(\vec{r}, t))|_{t=0} \neq \text{const.} \tag{A2}$$

We will now show that Eq. (A2) leads to a contradiction.

For subsystem K, the time-derivative of its current density $\vec{j}_K(\vec{r}, t)$ is

$$i\frac{\partial}{\partial t}\vec{j}_K(\vec{r}, t) = \langle\Psi_K(t)|[\hat{\vec{j}}_K(\vec{r}), \hat{H}_K(t)]|\Psi_K(t)\rangle,$$

where the current density operator is defined as

$$\hat{\vec{j}}_K(\vec{r}) = -\frac{1}{2i}\sum_s [\vec{\nabla}\hat{\psi}^+_{s,K}(\vec{r})\hat{\psi}_{s,K}(\vec{r}) - \vec{\nabla}\hat{\psi}_{s,K}(\vec{r})\hat{\psi}^+_{s,K}(\vec{r})].$$

Note that we have employed the conventional definition of the probability current, which has an opposite sign compared to the definition in Ref. 6. At $t = 0$, $\Psi_K(t = 0)$ and $\Psi_{K'}(t = 0)$ are identical, since we required that both unprimed and primed systems start from the same initial many-body wavefunction. Subtracting $\vec{j}_K$ from $\vec{j}'_K$ as in Ref. 6, we have

$$\begin{aligned} &i\frac{\partial}{\partial t}[\vec{j}_K(\vec{r}, t) - \vec{j}'_K(\vec{r}, t)]|_{t=0} \\ &\quad = -i\rho_K(\vec{r}, 0)\vec{\nabla}[u_{emb}(\vec{r}, 0) - u'_{emb}(\vec{r}, 0)], \end{aligned} \tag{A3}$$

where we have used the fact that $\{\rho_K(\vec{r}, t)\}$ is the same for both the primed and the unprimed systems at $t = 0$.

This article is copyrighted as indicated in the article. Reuse of AIP content is subject to the terms at: http://scitation.aip.org/termsconditions. Downloaded to IP: 66.67.101.221 On: Mon, 31 Mar 2014 14:59:43

As in Ref. 6, after applying the time-derivative l times to Eq. (A3), we obtain

$$\left(i\frac{\partial}{\partial t}\right)^{l+1}[\vec{j}_K(\vec{r},t)-\vec{j}'_K(\vec{r},t)]|_{t=0} = -i\rho_K(\vec{r},0)\vec{\nabla}\left[\left(i\frac{\partial}{\partial t}\right)^{l}(u_{emb}(\vec{r},t))-u'_{emb}(\vec{r},t)\Big|_{t=0}\right]. \tag{A4}$$

Based on the continuity theorem, for subsystem K we have

$$\frac{\partial}{\partial t}[\rho_K(\vec{r},t)-\rho'_K(\vec{r},t)] = -\vec{\nabla}\cdot[\vec{j}_K(\vec{r},t)-\vec{j}'_K(\vec{r},t)]. \tag{A5}$$

By applying ∂_t to Eq. (A5) $(l+1)$ times and with help from Eq. (A4), we obtain (after summing over all subsystems)

$$\frac{\partial^{l+2}}{\partial t^{l+2}}[\rho_{tot}(\vec{r},t)-\rho'_{tot}(\vec{r},t)]|_{t=0} = \vec{\nabla}\cdot[\rho_{tot}(\vec{r},0)\vec{\nabla}W(\vec{r})], \tag{A6}$$

where $W(\vec{r})$ is defined as

$$W(\vec{r}) \equiv \frac{\partial^l}{\partial t^l}[u_{emb}(\vec{r},t)-u'_{emb}(\vec{r},t)]|_{t=0},$$

which is non-zero due to our assumption. Green's theorem provides the identity

$$\int dr^3 W(\vec{r})\vec{\nabla}\cdot[\rho_{tot}(r,0)\vec{\nabla}W(\vec{r})] = -\int dr^3\rho_{tot}(\vec{r},0)[\vec{\nabla}W(\vec{r})]^2 + \oint \rho_{tot}(\vec{r},0)W(\vec{r})\cdot\hat{n}ds. \tag{A7}$$

In Eq. (A7), we assume that $\rho_{tot}(\vec{r},0)$ decays fast enough at the boundary to ensure the surface integral to be zero. Since $\int dr^3\rho_{tot}(\vec{r},0)[\vec{\nabla}W(\vec{r})]^2$ is non-zero, $\vec{\nabla}\cdot[\rho_{tot}(r,0)\vec{\nabla}W(\vec{r})]$ cannot be zero everywhere in space. Therefore, the left hand side of Eq. (A6) cannot be zero for order l, which means that $\rho_{tot}(\vec{r},t)$ and $\rho'_{tot}(\vec{r},t)$ will differ from each other at some point after $t=0$. This contradicts our initial assumption that $\rho_{tot}(\vec{r},t)=\rho'_{tot}(\vec{r},t)$ at all time, which proves that our assumption Eq. (A2) was incorrect. By proof of contradiction, we have thus shown that Eq. (A1) must hold for any order l at all time. Therefore $\rho_{tot}(\vec{r},t)$ determines $u_{emb}(\vec{r},t)$ up to a time-dependent constant.

[1] Y. Jiao, Z. Ding, and S. Meng, Phys. Chem. Chem. Phys. **13**, 13196 (2011).
[2] M. Moskovits, Rev. Mod. Phys. **57**, 783 (1985).
[3] J. Lee, P. Hernandez, J. Lee, A. O. Govorov, and N. A. Kotov, Nat. Mater. **6**, 291 (2007).
[4] E. Dalgaard and H. J. Monkhorst, Phys. Rev. A **28**, 1217 (1983); H. Sekino and R. J. Bartlett, Int. J. Quantum Chem., Quant. Chem. Symp. **26**, 255–265 (1984); K. L. Sebastian, Phys. Rev. B **31**, 6976 (1985); H. J. Monkhorst, Phys. Rev. A **36**, 1544 (1987); H. Koch and P. Jørgensen, J. Chem. Phys. **93**, 3333 (1990); J. F. Stanton and R. J. Bartlett, *ibid.* **98**, 7029 (1993); G. S. Latha and M. D. Prasad, *ibid.* **105**, 2972 (1996); C. Huber and T. Klamroth, *ibid.* **134**, 054113 (2011).
[5] J. Feist, S. Nagele, R. Pazourek, E. Persson, B. I. Schneider, L. A. Collins, and J. Burgdörfer, Phys. Rev. Lett. **103**, 063002 (2009).
[6] E. Runge and E. K. U. Gross, Phys. Rev. Lett. **52**, 997 (1984).
[7] P. Hohenberg and W. Kohn, Phys. Rev. **136**, B864 (1964).
[8] W. Kohn and L. J. Sham, Phys. Rev. **140**, A1133 (1965).
[9] J. P. Perdew and A. Zunger, Phys. Rev. B **23**, 5048 (1981); J. Messud, P. M. Dinh, P.-G. Reinhard, and E. Suraud, Phys. Rev. Lett. **101**, 096404 (2008).
[10] J. P. Perdew, R. G. Parr, M. Levy, and J. L. Balduz, Jr., Phys. Rev. Lett. **49**, 1691 (1982); M. Mundt and S. Kümmel, Phys. Rev. Lett. **95**, 203004 (2005).
[11] E. K. U. Gross and W. Kohn, Phys. Rev. Lett. **55**, 2850 (1985); **57**, 923(E) (1986); J. F. Dobson, Phys. Rev. Lett. **73**, 2244 (1994); G. Vignale, C. A. Ullrich, and S. Conti, *ibid.* **79**, 4878 (1997); J. F. Dobson, M. Bünner, and E. K. U. Gross, *ibid.* **79**, 1905 (1997); N. T. Maitra, K. Burke, and C. Woodward, *ibid.* **89**, 023002 (2002).
[12] C. Pisani, Phys. Rev. B **17**, 3143 (1978).
[13] A. R. Williams, P. J. Feibelman, and N. D. Lang, Phys. Rev. B **26**, 5433 (1982).
[14] M. Scheffler, C. Droste, A. Fleszar, F. Màca, G. Wachutka, and G. Borzel, Physica B **172**, 143 (1991).
[15] J. Bernholc, N. O. Lipari, and S. T. Pantelides, Phys. Rev. Lett. **41**, 895 (1978).
[16] J. E. Inglesfield, J. Phys. C: Solid State Phys. **14**, 3795 (1981).
[17] P. Cortona, Phys. Rev. B **44**, 8454 (1991).
[18] T. A. Wesolowski and A. Warshel, J. Phys. Chem. **97**, 8050 (1993).
[19] T. A. Wesolowski and J. Weber, Chem. Phys. Lett. **248**, 71 (1996).
[20] N. Govind, Y. A. Wang, A. J. R. da Silva, and E. A. Carter, Chem. Phys. Lett. **295**, 129 (1998).
[21] O. Roncero, M. P. de Lara-Castells, P. Villarreal, F. Flores, J. Ortega, M. Paniagua, and A. Aguado, J. Chem. Phys. **129**, 184104 (2008).
[22] O. Roncero, A. Zanchet, P. Villarreal, and A. Aguado, J. Chem. Phys. **131**, 234110 (2009).
[23] S. Fux, C. R. Jacob, J. Neugebauer, L. Visscher, and M. Reiher, J. Chem. Phys. **132**, 164101 (2010).
[24] J. D. Goodpaster, N. Ananth, F. R. Manby, and T. F. Miller III, J. Chem. Phys. **133**, 084103 (2010).
[25] F. R. Manby, M. Stella, J. D. Goodpaster, and T. F. Miller III, J. Chem. Theory Comput. **8**, 2564 (2012).
[26] M. H. Cohen and A. Wasserman, J. Stat. Phys. **125**, 1121 (2006).
[27] C. Huang, M. Pavone, and E. A. Carter, J. Chem. Phys. **134**, 154110 (2011).
[28] N. Govind, Y. A. Wang, and E. A. Carter, J. Chem. Phys. **110**, 7677 (1999).
[29] T. Klüner, N. Govind, Y. A. Wang, and E. A. Carter, Phys. Rev. Lett. **86**, 5954 (2001).
[30] T. Klüner, N. Govind, Y. A. Wang, and E. A. Carter, J. Chem. Phys. **116**, 42 (2002).
[31] P. Huang and E. A. Carter, J. Chem. Phys. **125**, 084102 (2006).
[32] T. A. Wesolowski, Phys. Rev. A **77**, 012504 (2008).
[33] S. Sharifzadeh, P. Huang, and E. A. Carter, Chem. Phys. Lett. **470**, 347 (2009).
[34] J. D. Goodpaster, T. A. Barnes, F. R. Manby, and T. F. Miller III, J. Chem. Phys. **137**, 224113 (2012).
[35] C. Huang and E. A. Carter, J. Chem. Phys. **135**, 194104 (2011).
[36] P. Huang and E. A. Carter, Annu. Rev. Phys. Chem. **59**, 261 (2008).
[37] C. R. Jacob and J. Neugebauer, "Subsystem density-functional theory," WIREs Comput. Mol. Sci. (published online, 2013).
[38] F. Libisch, C. Huang, and E. A. Carter, "Embedded Correlated Wavefunction Schemes: Theory and Applications," Accounts of Chemical Research (submitted).
[39] J. E. Inglesfield, J. Phys.: Condens. Matter **20**, 095215 (2008).
[40] J. E. Inglesfield, J. Phys.: Condens. Matter **23**, 305004 (2011).
[41] S. Corni and J. Tomasi, J. Chem. Phys. **114**, 3739 (2001).
[42] S. Jørgensen, M. A. Ratner, and K. V. Mikkelsen, J. Chem. Phys. **115**, 3792 (2001).
[43] D. Neuhauser and K. Lopata, J. Chem. Phys. **127**, 154715 (2007).
[44] D. Neuhauser, J. Chem. Phys. **135**, 204305 (2011).
[45] Y. Gao and D. Neuhauser, J. Chem. Phys. **137**, 074113 (2012).
[46] Y. Gao and D. Neuhauser, J. Chem. Phys. **138**, 181105 (2013).
[47] S. M. Morton and L. Jensen, J. Chem. Phys. **135**, 134103 (2011).
[48] D. Masiello and G. C. Schatz, Phys. Rev. A **78**, 042505 (2008).
[49] H. Chen, J. M. McMahon, M. A. Ratner, and G. C. Schatz, J. Phys. Chem. C **114**, 14384 (2010).
[50] M. E. Casida, in *Recent Advances in Density Functional Methods, Part I*, edited by D. P. Chong (World Scientific, Singapore, 1995).
[51] M. Petersilka, U. J. Gossmann, and E. K. U. Gross, Phys. Rev. Lett. **76**, 1212 (1996).
[52] M. E. Casida and T. A. Wesolowski, Int. J. Quantum Chem. **96**, 577 (2004).
[53] T. A. Wesolowski, J. Am. Chem. Soc. **126**, 11444 (2004).
[54] J. Neugebauer, J. Chem. Phys. **126**, 134116 (2007).

This article is copyrighted as indicated in the article. Reuse of AIP content is subject to the terms at: http://scitation.aip.org/termsconditions. Downloaded to IP: 66.67.101.221 On: Mon, 31 Mar 2014 14:59:43

[55]J. Neugebauer, J. Chem. Phys. **131**, 084104 (2009).
[56]M. Pavanello, J. Chem. Phys. **138**, 204118 (2013).
[57]S. Höfener, A. S. P. Gomes, and L. Visscher, J. Chem. Phys. **136**, 044104 (2012).
[58]G. Vignale, Phys. Rev. A **77**, 062511 (2008).
[59]R. van Leeuwen, Phys. Rev. Lett. **80**(6), 1280 (1998).
[60]Q. Wu and W. Yang, J. Chem. Phys. **118**, 2498 (2003).
[61]Q. Zhao, R. G. Parr, J. Chem. Phys. **98**, 543 (1993); Q. Zhao, R. C. Morrison, and R. G. Parr, Phys. Rev. A **50**, 2138 (1994).
[62]J. P. Perdew and Y. Wang, Phys. Rev. B **45**, 13244 (1992).
[63]C. Huang and E. A. Carter, Phys. Rev. B **84**, 165122 (2011).
[64]M. Fuchs and M. Scheffler, Comput. Phys. Commun. **119**, 67 (1999).
[65]X. Gonze, B. Amadon, P. Anglade, J.-M. Beuken, F. Bottin, P. Boulanger, F. Bruneval, D. Caliste, R. Caracas, M. Côté, T. Deutsch, L. Genovese, P. Ghosez, M. Giantomassi, S. Goedecker, D. Hamann, P. Hermet, F. Jollet, G. Jomard, S. Leroux, M. Mancini, S. Mazevet, M. Oliveira, G. Onida, Y. Pouillon, T. Rangel, G.-M. Rignanese, D. Sangalli, R. Shaltaf, M. Torrent, M. Verstraete, G. Zerah, and J. Zwanziger, Comput. Phys. Commun. **180**, 2582 (2009).
[66]T. Heaton-Burgess, F. A. Bulat, and W. Yang, Phys. Rev. Lett. **98**, 256401 (2007).
[67]J. Crank and P. Nicolson, Proc. Cambridge Philos. Soc. **43**, 50 (1947).
[68]A. Castro, M. A. L. Marques, and A. Rubio, J. Chem. Phys. **121**, 3425 (2004).
[69]M. A. Mosquera, D. Jensen, and A. Wasserman, Phys. Rev. Lett. **111**, 023001 (2013).
[70]D. Neuhauser, S. Pistinner, A. Coomar, X. Zhang, and G. Lu, J. Chem. Phys. **134**, 144101 (2011).
[71]C. A. Ullrich, U. J. Gossmann, and E. K. U. Gross, Phys. Rev. Lett. **74**, 872 (1995).
[72]G. Vignale and W. Kohn, Phys. Rev. Lett. **77**, 2037 (1996).
[73]S. Kümmel and L. Kronik, Rev. Mod. Phys. **80**, 3 (2008).

This article is copyrighted as indicated in the article. Reuse of AIP content is subject to the terms at: http://scitation.aip.org/termsconditions. Downloaded to IP: 66.67.101.221 On: Mon, 31 Mar 2014 14:59:43